

---

## Comparison of corrosion behaviour on 18% Ni 250 grade maraging steel under weld aged condition in NaCl and H<sub>2</sub>SO<sub>4</sub>

---

Rama Pavan Kumar Varma Indukuri\* and  
Rama Murty Raju Penmetsa

Department of Mechanical Engineering,  
SRKR Engineering College (A),  
Bhimavaram, Andhra Pradesh-534204, India  
Email: srkr.pavan.varma@gmail.com  
Email: dr.prmraju@gmail.com  
\*Corresponding author

Srinivasa Rao Chalamalasetti

Department of Mechanical Engineering  
Andhra University College of Engineering (A)  
Visakhapatnam, Andhra Pradesh-530003, India  
Email: prof.chsrao@andhrauniversity.edu.in

Rajesh Siriyala

Department of Mechanical Engineering,  
SRKR Engineering College (A),  
Bhimavaram, Andhra Pradesh-534204, India  
Email: dr.rajesh.mech@gmail.com

**Abstract:** Maraging steel sheets are used to manufacture components such as metal bellows that must withstand extreme temperatures and corrosion resistance in a variety of industries, including aircraft and aerospace. Laser beam welding is used to join maraging steel 250 plates with a thickness of 2 mm in this work. Under weld-aged conditions, the corrosion behaviour of 18% Ni MDN 250 grade maraging steel was examined in 1 M sulphuric acid (H<sub>2</sub>SO<sub>4</sub>) and 1 M sodium chloride (NaCl) solutions of equal concentrations. The potentiodynamic linear polarisation technique was used to conduct corrosion study. The results indicated that the corrosion rate increased with increasing laser power followed by welding speed and focal position. It is possible to improve the corrosion resistance of welded connections by adjusting the welding process parameters.

**Keywords:** maraging steel; similar welded joints; corrosion resistance; NaCl; H<sub>2</sub>SO<sub>4</sub>.

**Reference** to this paper should be made as follows: Indukuri, R.P.K.V., Penmetsa, R.M.R., Chalamalasetti, S.R. and Siriyala, R. (2024) 'Comparison of corrosion behaviour on 18% Ni 250 grade maraging steel under weld aged condition in NaCl and H<sub>2</sub>SO<sub>4</sub>', *Int. J. Materials Engineering Innovation*, Vol. 15, No. 1, pp.66–80.

**Biographical notes:** Rama Pavan Kumar Varma Indukuri is an Assistant Professor of the Department of Mechanical Engineering at S.R.K.R. Engineering, Bhimavaram, India. He received his Bachelor's degree from S.R.K.R. Engineering College and Master's degree from Adhiyamaan College of Engineering, Hosur, India. He is also a part time research scholar at Andhra University. His area of research is laser beam welding processes.

Rama Murty Raju Penmetsa received his MSc (Engineering) in Engineering from University College of Engineering, Sambalpur University, Burla. He obtained his PhD degree from Andhra University, Visakhapatnam. His areas of interest are fatigue and fracture mechanics, characterisation of materials, composites and finite element analysis. Currently, he is serving as a Professor in the Department of Mechanical Engineering at S.R.K.R. Engineering College, Bhimavaram, Andhra Pradesh. He has teaching experience of more than 20 years to UG/PG students of Mechanical Engineering, and he had published more than 40 research papers in various international/national journals and conferences to his credit.

Srinivasa Rao Chalamalasetti is a Professor in the Mechanical Engineering Department at Andhra University, Visakhapatnam, India. He obtained his PhD degree from Andhra University, Visakhapatnam, India. He has published around 270 research papers in various international journals and conferences proceedings. He is a member of various professional bodies like ISTE, IE, etc. His area of interest is manufacturing sciences, rapid prototyping, and robotics.

Rajesh Siriyala is a Professor in the Department of Mechanical Engineering at S.R.K.R. Engineering College, Bhimavaram, India. He received his Master's degree from R.V.R. & J.C. College of Engineering, Guntur. He obtained his PhD degree from Jawaharlal Nehru Technological University Kakinada, Kakinada. His areas of interest are characterisation of materials, tribology, and finite element analysis. He has published more than 40 research papers in various international/national journals and conferences.

---

## 1 Introduction

A key problem in the chemical processing sector is the corrosion of structural parts due to the aggressive chemical environment. The formation of alloying elements at temperatures more than 480°C is a peculiarity of the ultra-high-strength steels known as maraging. When compared to tempered martensitic alloy steels, maraging steels have a somewhat superior corrosion resistance (Sherif and Seikh, 2013; Sherif, 2014). When exposed to industrial and marine environments, maraging steel corrodes at a rate that is roughly half that of conventional steel. Maraging steels have a little improved corrosion resistance in salty and acidic environments. They are very strong because to the age hardening of a Fe-Ni martensitic matrix with minimal carbon content (Sastry et al., 2003). A consistent approach for welding maraging steel 250 with reduced HAZ and increased strength may be achieved by using laser beam welding. Precision industries like heat exchanger and valve production benefit from laser beam welding because of this (Fantoni et al., 2014; Van Rooyen et al., 2006) Even though laser beam weldments have good microstructural characteristics, thermal and mechanical properties, corrosion resistance is one of the most essential aspects in the assessment of maraging steel's service life. This metastable

martensite may change into ferrite and austenite if adequate time and temperature is supplied during the ageing procedure. Fusion welding methods such as laser and electron beam, plasma, and gas tungsten arc welding have shown maraging steels to be weldable. Numerous technical articles have been published (Tariq et al., 2010; Ramana et al., 2008; Quintino et al., 2007; Sakai et al., 2015; Young et al., 2007; Kose, 2020; Rajasekaran and Lakshminarayanan, 2021; Ragavendran et al., 2022; Singh and Shahi, 2022) on alloy design, material processing, thermomechanical treatments, welding, and strengthening processes, among other topics. These steels have emerged as viable alternatives to quenched and tempered steels in sophisticated technologies such as aerospace, nuclear energy, and gas turbines. They commonly come into contact with acids when cleaning, pickling, descaling, and acidifying. The majority of documented investigations focused on the corrosion of different metals and alloys in HCl and H<sub>3</sub>PO<sub>4</sub> solutions. Laser type effects on corrosion in 3.5% NaCl are clarified by Yan et al. (2019). The work has important practical implications since it assesses the effects of the multi-mode Nd:YAG laser and the quasi-basic mode slab CO<sub>2</sub> laser on the resistance to corrosion of welded joints. Using radioactive water with a pH as low as 6.5 with or without chloride ions, Bellanger and Rameau (1996) observed that the corrosion behaviour of maraging steel at the corrosion rate depends on pH and mediators persisting on the the material's surface favouring passivity. Corrosion behaviour of 18% Ni 250 maraging steel in corrosive media H<sub>2</sub>SO<sub>4</sub> was studied by Poornima et al. (2010), it was found that the annealed specimen corroded at a slower rate than the aged sample. To determine the optimal heat input range for maximising welding productivity, Yinhui et al. (2011) investigate the effects of high heat input on the microstructure and corrosion behaviour of simulated HAZs in 2,205 DSSs. Zhang et al. (2009) examined the link between solution heating temperature and mechanical attributes and pitting corrosion resistance to discover the optimal solution heating temperature for the researched specimen. On the other hand, the influence of annealing temperature on the microstructure, mechanical characteristics, and corrosion behaviour of this unique lean duplex stainless steel has been studied. Tan et al. (2009) studied the pitting corrosion resistance of super duplex stainless steels annealed at temperatures ranging from 1,030°C to 1,200°C without obvious precipitation of detrimental phases. Metallographic examinations, potentiodynamic polarisation tests, critical pitting temperature tests, scanning electron microscope and energy dispersive spectroscopy (SEM-EDS) analyses were performed by Kim et al. (2011) to clarify the effects of solution heat treatment and nitrogen incorporation in the shielding gas on the resistance to pitting corrosion of an HDSS weld. Two distinct types of DSS2304 (high-alloyed and low-alloyed) were welded using the Gleebe thermal-mechanical simulator, Tan et al. (2012) investigated, potentiostatic critical pitting temperature (CPT) in 1.0 M NaCl solution was used to examine the microstructure after the simulation and the resulting pitting corrosion resistance. However, it appears that no literature exists that discloses the corrosion behaviour of maraging steel in an acidic solution. The corrosion of maraging steel in NaCl and H<sub>2</sub>SO<sub>4</sub> acid media is the primary goal of this experiment. Specifically, the present study examines the impact of laser power, welding speed, and focus position on maraging steel sheet pitting corrosion rates. To determine pitting rate of corrosion, linear polarisation is used. An investigation on laser-beam welding of maraging steel 250 using NaCl and H<sub>2</sub>SO<sub>4</sub> solutions is the major focus of this study. The

corrosion resistance of maraging steel is investigated using the Potentiodynamic linear polarisation method. According to the results, laser power and the concentrations of H<sub>2</sub>SO<sub>4</sub> and NaCl in the corrosive medium increased, resulting in a rise in corrosion rates.

## 2 Welding procedure

Maraging steel sheets are used to make weld specimens using Nd:YAG laser beam welding machine that are 115 × 100 × 2 mm in size. Maraging steel 250-grade sheets chemical composition is shown in Table 1. Protective shielding and trailing gases are utilised with argon to prevent contamination from the outside environment. Table 2 shows the values of the process parameters and their respective levels which are chosen following a feasibility analysis. The EDAX Analysis in order to identify the elements and its weight percentages present in the maraging steel (MDN 250) are shown in Figure 1.

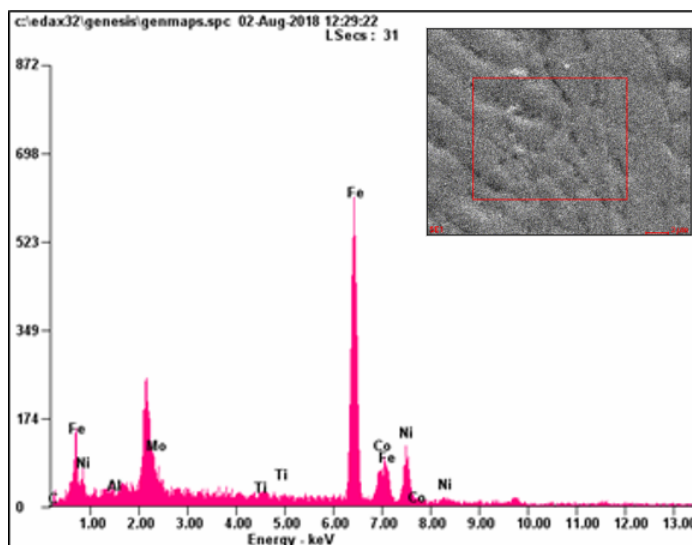
**Table 1** Chemical composition of maraging steel (MDN250)

Element	Ni	C	Co	Mo	Ti	Al	Mn	Fe
Wt %	18.9	0.02	8.1	4.9	0.4	0.15	0.04	Balance

**Table 2** Process variables and their levels

Parameters	Notation	Units	Level 1	Level 2	Level 3	Level 4
Laser power	LP	kW	1	1.33	1.66	2
Welding speed	WS	m/min	0.6	1.2	1.8	2.4
Focal position	FP	mm	-1	0	1	2

**Figure 1** EDAX Analysis for maraging steel 250 (see online version for colours)



### 3 Measurement of pitting corrosion rate

When maraging steel is exposed to varied conditions, the welds are susceptible to pitting corrosion. An exposed environment's kind, concentration, and length of exposure are all factors in pitting corrosion rate. The next few paragraphs will detail the steps necessary to get a good sample ready for rate of pitting corrosion.

#### 3.1 Preparation of specimens of maraging steel

All specimens were cut to an apparent size of 2 mm × 2 mm. These specimens were scraped away using emery sheets ranging in grade from 120 to 1,000. The specimens were cut using wire cut EDM with an accuracy of ±0.0001 mm. After degreasing with acetone, washing with double distilled water, and drying, it was immersed in corrosion attack. Figure 2 shows the corrosion test specimen.

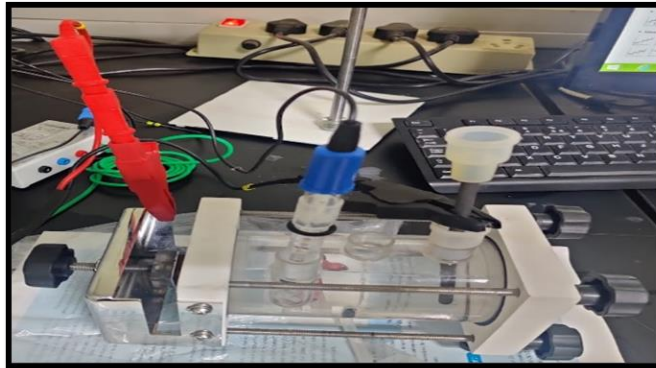
**Figure 2** Corrosion test specimen (see online version for colours)



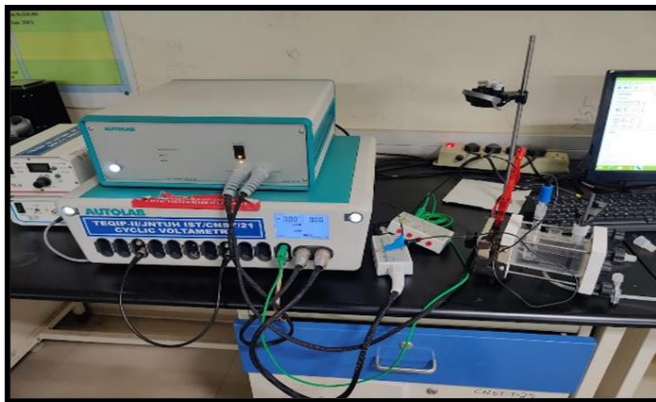
#### 3.2 Preparation of corrosive medium

For corrosion inhibition investigations, 1M NaCl solution and 1M H<sub>2</sub>SO<sub>4</sub> was prepared by measuring 54.44 gm of NaCl and 54.03 ml of H<sub>2</sub>SO<sub>4</sub> solution was placed in 1 litre volumetric flask and then filled the flask with double distilled water up to the graduation mark. Figure 3 illustrates the TAFEL studies and pitting corrosion setup.

**Figure 3** (a) Photograph shows TAFEL studies (b) Pitting corrosion setup (see online version for colours)



(a)



(b)

#### 4 Potentiodynamic studies

To perform potentiodynamic corrosion investigations, an electrochemical corrosion analyser of CH Instruments was used. Since the maraging steel is more vulnerable to chloride environments, the samples are evaluated in 1 M NaCl and 1 M H<sub>2</sub>SO<sub>4</sub> solution. Three electrodes are used in this experiment such as the weldment is a working electrode, a platinum electrode is a counter electrode, and a saturated calomel electrode via capillary probe is a reference electrode. Total surface area exposed to solution during testing is 20 mm, which includes the weld cross section and a 2 × 2 mm region next to it. The working electrode was exposed to the corrosive atmosphere for 15 minutes while maintain an open circuit potential (OCP). Potentiodynamic polarisation curves were generated by switching the electrode potential from cathodic to anodic. Extrapolation of the TAFEL plots was used to get the corrosion potential E<sub>Corr</sub> and the corrosion current I<sub>Corr</sub>.

#### 4.1 Tafel polarisation studies

When subjected to the same quantities of 1 M sodium chloride (NaCl) and 1 M sulphuric acid (H<sub>2</sub>SO<sub>4</sub>) for the same amount of time, 1 cm<sup>2</sup> areas of finely polished weld-aged maraging steel were measured for their OCP. The open circuit potential is calculated by averaging the measurements from the past five minutes. Recorded potentiodynamic current potential curves were obtained by conducting OCP scans of the specimens at a scan rate of 1 millivolt per second.

#### 4.2 Procedure for corrosion studies

In the beginning, distilled water is used to clean the electrochemical cell (the test specimen in the tube), and then filtered electrolytes of 1 M NaCl and 1 M H<sub>2</sub>SO<sub>4</sub> are used to rinse the cell. The electrochemical cell is filled with around 100 cc of filtered electrolyte. All of the components of the electrode assembly have been inserted into the cell. An adjustment is made to the reference electrode (the standard calomel electrode) to ensure that its tip is as close as possible to an exposed part of a working electrode's electrode surface (test specimen). Additionally, the cell has a platinum electrode. The AUTOLAB/PGSTAT12 has now been linked to the cell assembly. Counter electrode is black, working electrode is red, and reference electrode is blue. Using these colours, the plugs have been linked. The sample has been in contact with an electrolytic media for three hours now. It is only when the main switch of the potentiostat was pressed that the electrode potential begins to fluctuate until equilibrium is reached. After a period of time, the potential is almost imperceptibly stable and does not vary. An open circuit potential is defined as a constant voltage shown on the monitor ( $E_{rest}$ ). It is now possible to collect polarisation data using the available equipment. The potential is scanned cathodically so that it is equal to the  $E_{rest}$  minus the cutoff potential.  $E$  versus  $\log I$  plots of potential ( $E$ ) and current ( $I$ ) are presented on the monitor at varied intervals. Scans are reversed after exceeding the cathodic threshold. In the same way, anodic polarisation data is gathered as well. Upon reaching  $E_{rest}$ , the cell is separated from the potentiostat and the scan is repeated one more before being terminated. The Tafel diagram is based on the reported data (current vs potential data). Tafel plot techniques are used to analyse corrosion current, polarisation resistance, and Tafel slopes.

#### 4.3 Linear polarisation technique

For linear polarisation, the Tafel extrapolation technique is used. Polarised resistance is used to quantify total rate of corrosion, which is given as millimetre per year (mpy). It is possible to assess polarisation resistance in a matter of minutes, on average less than 10 minutes. In order to test the polarisation resistance, a voltage range that is extremely near to the corrosion potential is scanned. This voltage range is typically 25 mV or less around  $E_{corr}$ . It's possible to see the relationship between the generated current and potential on a graph. The following equation links the corrosion current,  $I_{corr}$ , to the plot's slope:

$$\frac{\Delta E}{\Delta I} = \frac{\beta_a \beta_c}{2.3 I_{corr} (\beta_a + \beta_c)} \quad (1)$$

wherein

$$Rp = \Delta E / \Delta I$$

wherein  $\Delta E$  is expressed in volts and  $\Delta I$  in  $\mu A$ .

Resistance is a measurable quantity, called as slope. The anode Tafel constant is a  $\beta_a$  the cathode Tafel constant is  $\beta_c$ . The measurement units for these constants are expressed in volts per decade of current.

$I_{corr}$  = corrosion current,  $\mu A$

$$I_{corr} = \frac{\beta_a \beta_c}{2.3 I_{corr} (\beta_a + \beta_c)} \frac{\Delta E}{\Delta I} \quad (2)$$

The rate of corrosion could be calculated from the corrosion current using the following equation:

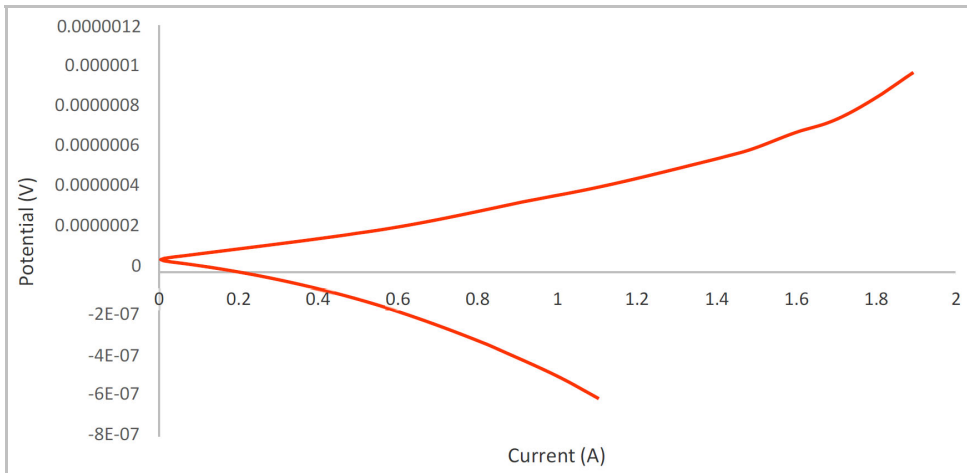
$$\text{Rate of corrosion (mpy)} = 0.131 (I_{corr}) (\text{Eq. Wt}) / \rho \quad (3)$$

wherein Eq. Wt is the equivalent weight of the component that causes corrosion and  $\rho$  – density,  $g/cm^3$ .

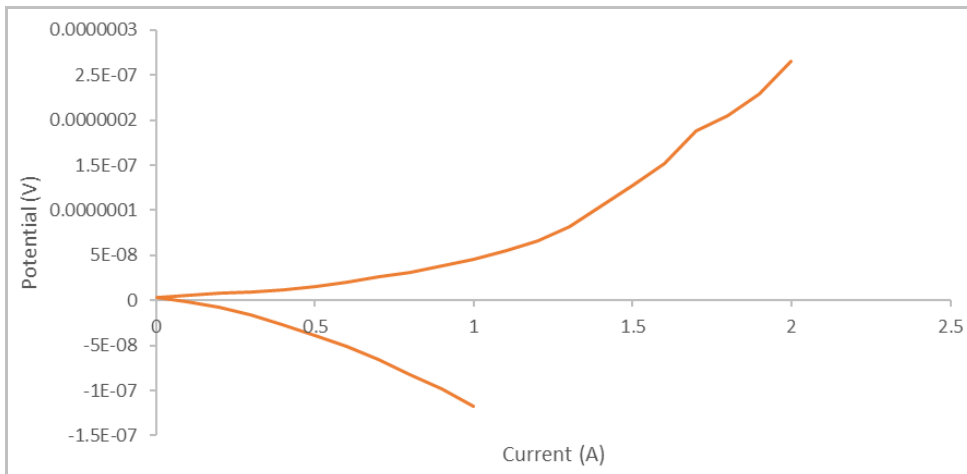
## 5 Electrochemical measurement

### 5.1 Effect of immersion time

Figures 4(a) and 4(b) show the polarisation curves for maraging steel specimens of 250 grade immersed in 1 M  $H_2SO_4$  and 1 M NaCl solution for 10 minutes at room temperature. It is possible to calculate the corrosion potential ( $E_{corr}$ ), the corrosion current density ( $J_{corr}$ ), and the polarisation resistance ( $R_p$ ) using the linear polarisation curves as a reference. It is clear from the polarisation curve that the cathodic current of the maraging steels decreases in negative value as the potential increases until the current achieves its minimal value at the corrosion current density,  $J_{corr}$ . Graphing the extrapolation of the cathodic and anodic Tafel slopes to the  $E_{corr}$  resulted in the corrosion current density,  $J_{corr}$ . According to the polarisation diagram [Figures 4(a) and 4(b)], increasing immersion duration causes an increase in the values of anodic currents  $J_{corr}$  as well as a shift in the values of cathodic currents  $E_{corr}$ . From the curves, polarisation resistance ( $R_p$ ) decreases with increasing immersion time. As a result, it may be said that the aggressive action of sulphuric acid raises the rate of corrosion in maraging steels as immersion duration rises. Because sulphuric acid is constantly attacking the steel surface, the production of oxides is hindered. It is possible to increase the applied potential in a positive direction even more.

**Figure 4** Model Tafel plot for (a) 1 M NaCl and (b) 1 M H<sub>2</sub>SO<sub>4</sub> (see online version for colours)

(a)



(b)

## 6 Influence of process parameters on pitting rate of corrosion

Welded pitting rate of corrosion and interactions for such range of factors involved to study and may be predicted using the mathematical model created above by replacing their parameters in encoded. Weld pitting corrosion rates for H<sub>2</sub>SO<sub>4</sub> solution may be calculated and displayed using these models (see Figure 5) to see how process factors affect these rates. The pitting corrosion rate reduces from 0.6 m/min of welding speed to 2.4 m/min, as shown in Figure 5. From 1 kW to 2 kW of laser power, the rate of pitting corrosion rises continually. As the focus distance grows, so does the rate of pitting corrosion. The increase (or) decrease in the corrosion rate of laser beam welding in 1 M H<sub>2</sub>SO<sub>4</sub> may be attributed due to the attack by sulphuric acid at grain boundaries

(Poornima et al., 2010). Because corrosion is a serious problem in these areas. Corrosion rates may be more (or) less depending on the quantity of inter-metallic precipitation at the grain boundary.

**Figure 5** Main Effect plot of corrosion resistance in H<sub>2</sub>SO<sub>4</sub> solution (see online version for colours)

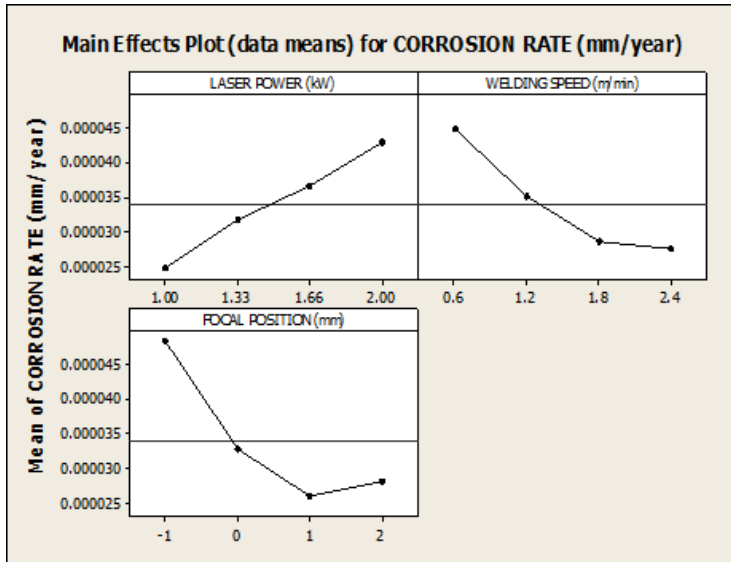
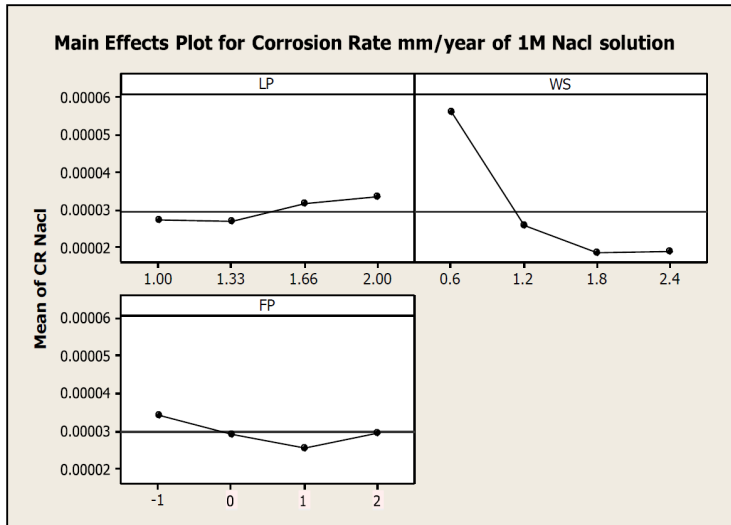


**Figure 6** Main effect plot of corrosion resistance in NaCl solution (see online version for colours)



The pitting corrosion rate reduces from 0.6 m/min of welding speed to 2.4 m/min, as shown in Figure 6. Pitting corrosion rates rise steadily with increasing laser power, from 1 kW to 2 kW, The rate of pitting corrosion falls from a focused distance of  $-1$  mm to a distance of 1 mm, and then increases to a focal distance of 2 mm. In 1 M NaCl, the quantity of retained austenite may be responsible for an increase (or) decrease in the corrosion rate of laser beam welding joint. In general, the propensity to create retained austenite increases as the quantity of molybdenum (Mo) alloying element rises. For this reason, it is possible that Mo content has an effect on pitting resistance (Seikh et al., 2021).

## 7 Results and discussion

To find the response's maximum and lowest values, surface charts are useful. The peak of the surface plot depicts the response's greatest value, while the bottom of the surface plot's depicts response's smallest value. The bottom of the response surface indicates the lowest pitting corrosion rate. The peak surface response for NaCl solution in Figure 7(a) displays the 3D surface graph for pitting rate of corrosion produced the regression model, assumed as a laser power of 1 kW to 2 kW and welding speed of 0.6 m/min to 2.4 m/min to get the optimal corrosion rate. The figure shows that when laser power rises, the rate of pitting corrosion rises as well. The maximum pitting corrosion rate may be determined from the welding speed, which indicates that the slower the welding speed, the better.

The optimum may be obtained between laser power and welding speed. To obtain the pitting response for the rate of corrosion a laser power of 1 kW to 2 kW and focal position of  $-1$  mm to 2 mm [see Figure 7(b)] was assumed. The response graph shows that the twisted plane is in the centre of attention. Pitting corrosion is more prevalent when laser power is at its highest.

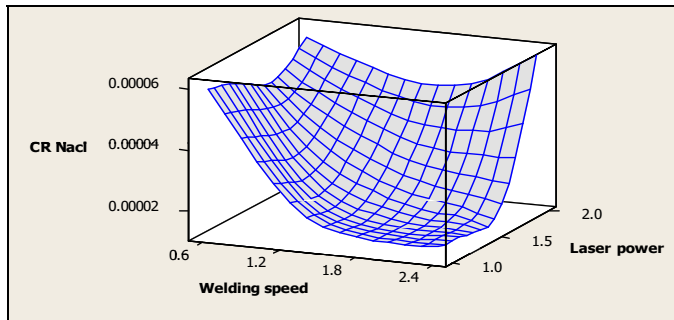
For the response pitting corrosion rate, shown in Figure 7(c), the 3D response surface graph was generated by assuming welding speeds between 0.6 m/min and 2.4 m/min and a focal position of  $-1$  mm to 2 mm. The model's interaction may be observed in the twisted plane of the surface plot. Pitting corrosion is at its lowest level when the welding speed is reduced, as can be seen from the reaction graph. The pitting corrosion rate is lowest when the focal position is between  $-1$  mm and 2 mm.

Figure 7(d) indicates 3D surface response graph for the pitting rate of corrosion was generated by assuming a laser power of 1 kW to 2 kW and welding speed of 0.6 m/min to 2.4 m/min. The highest surface response determines the pitting rate of corrosion that is optimal. The surface graph shows that higher welding speeds and lower laser power result in less pitting corrosion. Additionally, decreased welding speed and increased laser power result in increased pitting corrosion.

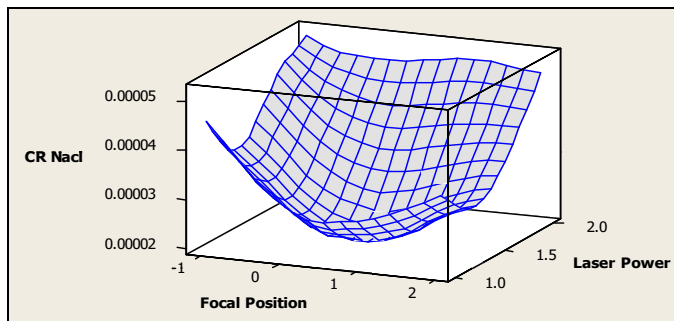
Figure 7(e) shows the 3D surface response graph for pitting rate of corrosion received as laser power 1 kW to 2 kW and focal position of  $-1$  mm to 2 mm. The distorted plane of surface plot shows the interaction. The graph shows that when the laser power and Focal position are placed to the middle level, the pitting rate of corrosion of the laser beam butt joint is the lowest.

Figure 7(f) shows the 3D surface response plot for pitting rate of corrosion generated by assuming a welding speed of 0.6 m/min to 2.4 m/min and focal position of 1 mm to 2 mm. The warped plane surface graph contains the interaction. The response graph shows the pitting rate of corrosion is lowest when welding speed is high and the focal position is in the middle. The surface plots shows that the best pitting corrosion rate is attained with greater laser power and lower welding speed.

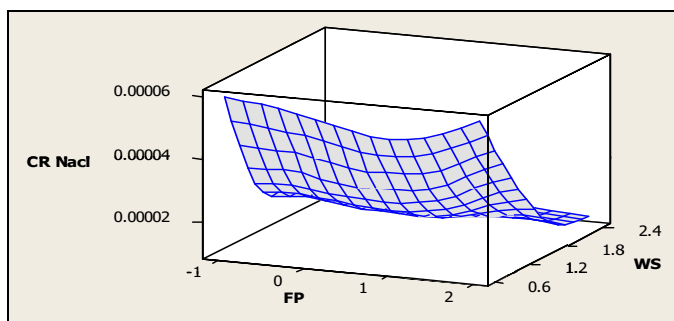
**Figure 7** (a) Surface plot (laser power and welding speed) (b) Surface plot (laser power and focal position) (c) Surface plot (welding speed and focal position) (d) Surface graph H<sub>2</sub>SO<sub>4</sub> solution (laser power vs. welding speed) (e) Surface plot H<sub>2</sub>SO<sub>4</sub> solution (laser power vs. focal position) (f) Surface plot H<sub>2</sub>SO<sub>4</sub> solution (welding speed vs. focal position) (see online version for colours)



(a)

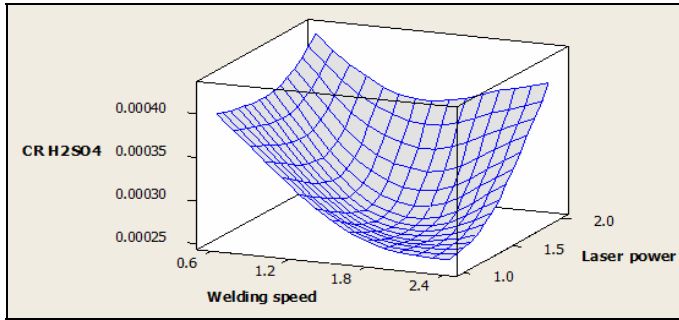


(b)

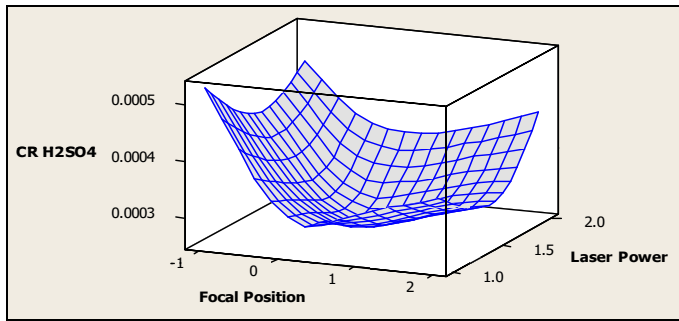


(c)

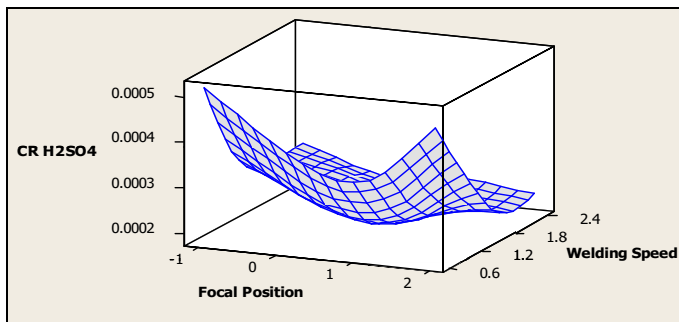
**Figure 7** (a) Surface plot (laser power and welding speed) (b) Surface plot (laser power and focal position) (c) Surface plot (welding speed and focal position) (d) Surface graph H<sub>2</sub>SO<sub>4</sub> solution (laser power vs. welding speed) (e) Surface plot H<sub>2</sub>SO<sub>4</sub> solution (laser power vs. focal position) (f) Surface plot H<sub>2</sub>SO<sub>4</sub> solution (welding speed vs. focal position) (continued)



(d)



(e)



(f)

## 8 Conclusions

In the present work, LBW butt joint was done on 2 mm thick maraging steel under varied welding conditions. Corrosion tests are performed on the welded joints in corrosive media using linear polarisation technique. The experimental findings allow us to draw the following inferences:

- 1 TAFEL plots are drawn by measuring pitting corrosion rate in both 1 M H<sub>2</sub>SO<sub>4</sub> and 1M NaCl solutions on maraging steel welded joints.
- 2 Based on the input parameters of laser power (1.33 kW), welding speed (1.8 m/min), and focal position (2 mm), the lowest pitting rate of corrosion attained is 0.00002533 mm/year for an H<sub>2</sub>SO<sub>4</sub> solution.
- 3 Based on the input parameters of laser power (1.33 kW), welding speed (2.4 m/min), and focal position (1 mm), the lowest pitting rate of corrosion attained is 0.0000131 mm/year for NaCl solution.
- 4 By comparing both solutions the order of corrosion severity is more for 1 M H<sub>2</sub>SO<sub>4</sub> when compared to 1 M NaCl solution. The NaCl solution may have encouraged Mo to increase more protective layer.
- 5 According to the surface plots, input parameters have a significant impact on pitting corrosion rate.

## References

- Bellanger, G. and Rameau, J.J. (1996) 'Effect of slightly acid pH with or without chloride in radioactive water on the corrosion of maraging steel', *Journal of Nuclear Materials*, Vol. 228, No. 1, pp.24–37.
- Fanton, L., Abdalla, A.J. and Lima, M.S.F. (2014) 'Heat treatment and Yb-fiber Laser welding of a maraging steel', *Welding Journal*, Vol. 93, pp.362–368.
- Kim, S.T., Jang, S.H., Lee, I.S. and Park, Y.S. (2011) 'Effects of solution heat-treatment and nitrogen in shielding gas on the resistance to pitting corrosion of hyper duplex stainless steel welds', *Corrosion Science*, Vol. 53, No. 5, pp.1939–1947.
- Kose, C. (2020) 'Characterization of weld seam surface and corrosion behavior of laser-beam-welded AISI 2205 duplex stainless steel in simulated body fluid', *Journal of Materials Science*, Vol. 55, No. 36, pp.17232–17254.
- Poornima, T., Jagannatha, N. and Nityananda, S. (2010) 'Studies on corrosion of annealed and aged 18 Ni 250 grade maraging steel in sulphuric acid medium', *Portugaliae Electrochimica Acta*, Vol. 28, No. 3, pp.173–188.
- Quintino, L., Costa, A., Miranda, R., Yapp, D., Kumar, V. and Kong, C.J. (2007) 'Welding with high power fiber lasers – a preliminary study', *Materials & Design*, Vol. 28, No. 4, pp.1231–1237.
- Rajasekaran, R. and Lakshminarayanan, A.K. (2021) 'Probing the stress corrosion cracking resistance of laser beam welded AISI 316LN austenitic stainless steel', *Proceedings of the Institution of Mechanical Engineers, Part C: Journal of Mechanical Engineering Science*, Vol. 235, No. 17, pp.3299–3317.
- Ragavendran, M., Toppo, A. and Vasudevan, M. (2022) 'SCC behaviour of laser and hybrid laser welded stainless steel weld joints', *Materials Science and Technology*, Vol. 38, No. 5, pp.281–298.
- Ramana, P.V., Reddy, G.M. and Mohandas, T. (2008) 'Microstructure, hardness and residual stress distribution in maraging steel gas tungsten arc weldments', *Science and Technology of Welding and Joining*, Vol. 13, No. 4, pp.388–394.
- Sakai, P.R., Lima, M.S.F., Fanton, L., Gomes, C.V., Lombardo, S., Silva, D.F. and Abdalla, A.J. (2015) 'Comparison of mechanical and microstructural characteristics in maraging 300 steel welded by three different processes: LASER, PLASMA and TIG', *Procedia Engineering*, Vol. 114, pp.291–297.

- Sastry, K.Y., Narayanan, R., Shamantha, C.R., Sundaresan, S., Seshadri, S.K., Radhakrishnan, V.M. and Sundararajan, S. (2003) 'Stress corrosion cracking of maraging steel weldments', *Materials Science and Technology*, Vol. 19, No. 3, pp.375–381.
- Seikh, A.H., Halfa, H. and Soliman, M.S. (2021) 'Effect of molybdenum content on the corrosion and microstructure of low-Ni, co-free maraging steels', *Metals*, Vol. 11, No. 6, p.852.
- Sherif, E.S.M. and Seikh, A.H. (2013) 'Effects of immersion time and 5-phenyl-1H-tetrazole on the corrosion and corrosion mitigation of cobalt free maraging steel in 0.5 M sulfuric acid pickling solutions', *Journal of Chemistry*, Vol. 49823, pp.1–7.
- Sherif, E.S.M. (2014) 'Corrosion inhibition in 2.0 M sulfuric acid solutions of high strength maraging steel by aminophenyl tetrazole as a corrosion inhibitor', *Applied Surface Science*, Vol. 292, pp.190–196.
- Singh, J. and Shahi, A.S. (2022) 'Microstructure and corrosion behavior of duplex stainless-steel electron beam welded joint', *Journal of Materials Science*, Vol. 57, No. 20, pp.9454–9479.
- Tan, H., Jiang, Y., Deng, B., Sun, T., Xu, J. and Li, J. (2009) 'Effect of annealing temperature on the pitting corrosion resistance of super duplex stainless steel UNS S32750', *Materials Characterization*, Vol. 60, No. 9, pp.1049–1054.
- Tan, H., Wang, Z., Jiang, Y., Yang, Y., Deng, B., Song, H. and Li, J. (2012) 'Influence of welding thermal cycles on microstructure and pitting corrosion resistance of 2304 duplex stainless steels', *Corrosion Science*, Vol. 55, pp.368–377.
- Tariq, F., Baloch, R.A., Ahmed, B. and Naz, N. (2010) 'Investigation into microstructures of maraging steel 250 weldments and effect of post-weld heat treatments', *J. Mater. Eng. Perform.*, Vol. 19, No. 2, pp.264–273.
- Van Rooyen, C., Burger, H.P. and Kazadi, B.P. (2006) *Comparison of CO<sub>2</sub> and Nd:YAG Laser Welding of Grade 250 Maraging Steel*, IIW Doc. II-A.173-206.
- Yan, S., Shi, Y., Liu, J. and Ni, C. (2019) 'Effect of laser mode on microstructure and corrosion resistance of 316L stainless steel weld joint', *Optics & Laser Technology*, Vol. 113, pp.428–436.
- Yinhui, Y., Biao, Y. and Jie, L. (2011) 'The effect of large heat input on the microstructure and corrosion behavior of simulated heat affected zone in 2205 duplex stainless steel', *Corrosion Science*, Vol. 53, No. 11, pp.3756–3763.
- Young, M.C., Tsay, L.W., Shin, C.S. and Chan, S.L.I. (2007) 'The effect of short time post-weld heat treatment on the fatigue crack growth of 2205 duplex stainless steel welds', *International Journal of Fatigue*, Vol. 29, No. 12, pp.2155–2162.
- Zhang, L., Zhang, W., Jiang, Y., Deng, B., Sun, D. and Li, J. (2009) 'Influence of annealing treatment on the corrosion resistance of lean duplex stainless steel 2101', *Electrochimica Acta*, Vol. 54, No. 23, pp.5387–5392.